Available online at www.sciencedirect.com
ScienceDirect
Journal of Magnetism and Magnetic Materials 316 (2007) 306–312
Journal of magnetism and magnetic materials
www.elsevier.com/locate/jmmm

Helimagnetism and weak ferromagnetism in edge-shared chain cuprates

S.-L. Drechsler[a,*], J. Richter[b], R. Kuzian[c], J. Málek[d], N. Tristan[a], B. Büchner[a], A.S. Moskvin[e], A.A. Gippius[f], A. Vasiliev[f], O. Volkova[f], A. Prokofiev[g], H. Rakoto[h], J.-M. Broto[h], W. Schnelle[i], M. Schmitt[i], A. Ormeci[i], C. Loison[i], H. Rosner[i]

[a]*Leibniz-Institut für Festkörper- und Werkstoffforschung IFW Dresden, Postfach 270116, D-01171 Dresden, Germany*
[b]*Institut für Theoretische Physik, Universität Magdeburg, D-39016 Magdeburg, Germany*
[c]*Institute for Problems of Materials Science, Kiev, Ukraine*
[d]*Institute of Physics, ASCR, Prague, Czech Republic*
[e]*Ural State University, 620083 Ekaterinburg, Russia*
[f]*Moscow State University, 119992 Moscow, Russia*
[g]*Institut für Festkörperphysik, Technische Universität Wien, A-1040 Wien, Austria*
[h]*Laboratoire National de Champs Magnétiques Pulsés, 31432 Toulouse, France*
[i]*Max-Planck-Institut für Chemische Physik fester Stoffe, D-01187 Dresden, Germany*

Available online 1 April 2007

Abstract

The present understanding of a novel growing class of chain cuprates with intriguing magnetic properties is reviewed. Among them, several undoped edge-shared CuO_2 chain compounds show at low temperature a clear tendency to helicoidal magnetical ordering with acute pitch angles and sometimes also to weak ferromagnetism. Our analysis is based on the isotropic 1D frustrated J_1-J_2 Heisenberg model with ferromagnetic (FM) 1st neighbor and antiferromagnetic 2nd neighbor exchange. The achieved assignment is supported by microscopic calculations of the electronic and magnetic structure. We consider $Na(Li)Cu_2O_2$, $LiVCuO_4$ as the best studied helimagnets, Li_2ZrCuO_4 and other systems close to a FM quantum critical point, as well as Li_2CuO_2 with FM inchain ordering. The interplay of frustrated inchain couplings, anisotropy and interchain exchange is discussed.

PACS: 74.72.Jt; 76.60.−k; 75.10.−b; 75.10.Pq

Keywords: Edge-shared cuprate chain; Quantum helix; Weak ferromagnetism; High-field magnetization

1. Introduction—brief historical remarks

Undoped edge-shared CuO_2 chain compounds (see, e.g., Figs. 1–4) exhibit a surprisingly large variety of magnetic ground states. Thus, below $T_N \approx 9$ K the prototypical Li_2CuO_2 [1,2] shows a commensurate Néel state dominated by antiferromagnetic (AFM) interchain coupling but accompanied also by a ferromagnetic (FM) inchain ordering and below 2.5 K a not yet understood canted magnetic structure [2]. In contrast, the closely related $LiVCuO_4$ [3,4], $LiCu_2O_2$ [5–9] $NaCu_2O_2$ [9,11–13] show incommensurate (IC) magnetic structures along the chain direction b below $T_h \approx 3$, 24, and 13 K, respectively, which represent the first long-sought [14] helices with acute pitch angles for quantum localized spin-$\frac{1}{2}$ systems. Such a special helical assignment was achieved and accepted only stepwise after the synthesis of these compounds 15–20 years ago and first not very meaningful measurements. At that time, guided by the observed maxima in the magnetic susceptibility $\chi(T)$ and the specific heat c_p at relatively low T, nearly ideal (quasi)-1D Heisenberg AFM behavior with a standard Néel-ordering below due to remaining interchain coupling was suggested [15–20]. It can be described by the Hamiltonian

$$\mathscr{H} = \sum_{ij,\alpha\beta} J_{ij}^{\alpha\beta} S_i^{\alpha} S_j^{\beta} + \mathbf{D}_{ij} \cdot (\mathbf{S}_i \times \mathbf{S}_j), \tag{1}$$

*Corresponding author. Tel.: +49 351 4659 384; fax: +49 351 4659 490.
E-mail address: drechsler@ifw-dresden.de (S.-L. Drechsler).

0304-8853/$ - see front matter © 2007 Elsevier B.V. All rights reserved.
doi:10.1016/j.jmmm.2007.03.200

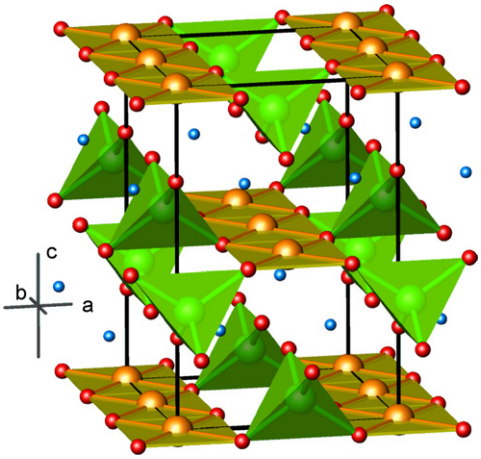

Fig. 1. Crystal structure of $LiCuVO_4$ with ideal planar CuO_2 chains $\parallel b$. Atomic notation: large orange ○—Cu, small red ○—O, large green ○—V, and small blue ○—Li.

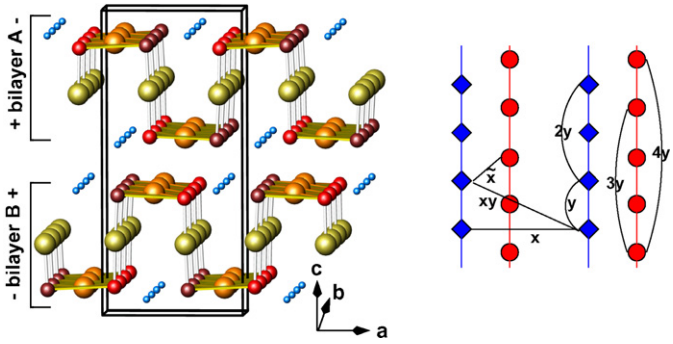

Fig. 2. The DC structure of $Na(Li)Cu_2O_2$. Crystal structure with a DC in the center (left panel). Atomic notation the same as in Fig. 1; large grey ○—the magnetically non-active Cu(1+) ions, nonequivalent O in small red and brown ○. Projected bilayer onto the (a,b) plane with two double-chain's (right panel). ◆ and • denote Cu sites in different planes. The main exchange paths are denoted by off-chain lines (a shortened notation $J_3 \equiv J_{3y}$ and $J_4 \equiv J_{4y}$ is used in the text).

where i and j run over pairs of nearest neighbor (NN) and next-nearest neighbor (NNN) CuO_4 plaquettes and the last antisymmetric exchange term (Dzyaloshinski–Moriya (DM)) allowed by symmetry only for certain non-ideal systems under consideration, will be at first ignored. The general Hamiltonian $\mathscr{H}$ applied to a real chain compound exhibits a hierarchy of isotropic and anisotropic couplings with the leading terms given by isotropic NN and NNN in-chain exchange denoted as J_1 and J_2, respectively, below. At the next step the possible presence of IC magnetic ground states with helical structures and anisotropic symmetric exchange [17,18,20] was realized. By neutron diffraction for $LiCuVO_4$ and $Na(Li)Cu_2O_2$ [3–5,11] the corresponding propagation vectors near $\frac{1}{4}$: $\zeta = 0.234$, 0.227, and 0.1724, respectively, (in units of the reciprocal lattice vector $2\pi/b$ of a single chain) and nonequivalent Bragg reflexes near integer values $k \pm \zeta$ have been found. Thus, two of the related pitch angles $\phi = 84.2\ (83.6 \pm 0.6)^\circ$, 81.7°, 62.1° are close to $\pi/2$. However, strictly speaking, the acute pitch angle assignment from neutron diffraction alone is

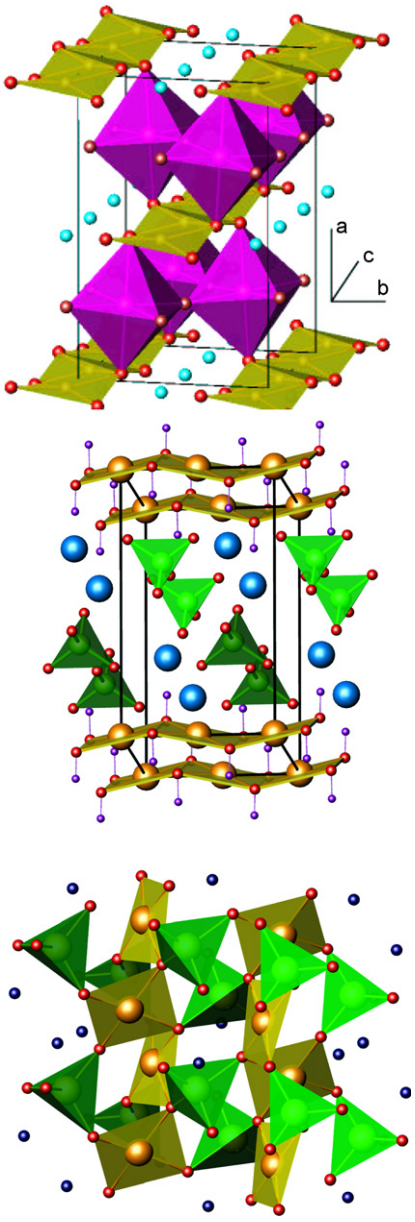

Fig. 3. The crystal structure of Li_2ZrCuO_4 with buckled chains $\parallel c$. Notation as in Figs. 1 and 2; Cu—bright olive-green ○ Zr—bright ○ inside the magenta corner-shared VO_6 octahedra (upper panel). Middle panel: the same for the buckled chain compound $Pb_2[CuSO_4(OH)_2]$. Pb(H)—large (small) blue ○, S—green ○ inside the green SO_4 tetrahedra. Lower panel: the isomorphic structure of the two strongly buckled and asymmetric corner-shared CuO_3 chain compounds $Rb(Cs)_2Cu_2Mo_3O_{12}$. Mo—green ○ inside the green MO_4 tetrahedra, Rb(Cs)—small blue ○.

not unique [21]. The corresponding alternative set to ζ symmetric to $\frac{1}{4}$: $\zeta' = 0.266$, 0.273, and 0.3276, leads to obtuse pitch angles $\phi' = 95.76\ (96.4)^\circ$, etc., i.e. AFM J_1 values would also fit the neutron diffraction data. An analysis of additional data such as inelastic neutron scattering, $\chi(T)$, and high-field magnetization data or convincing theoretical arguments [4,6–8,12,22,23] are necessary to settle the FM sign (i.e. $J_1 < 0$). In $Na(Li)Cu_2O_2$, in principle, a significant AFM double-chain (dc) exchange $\tilde{J}$ (see Fig. 2, right panel) might affect

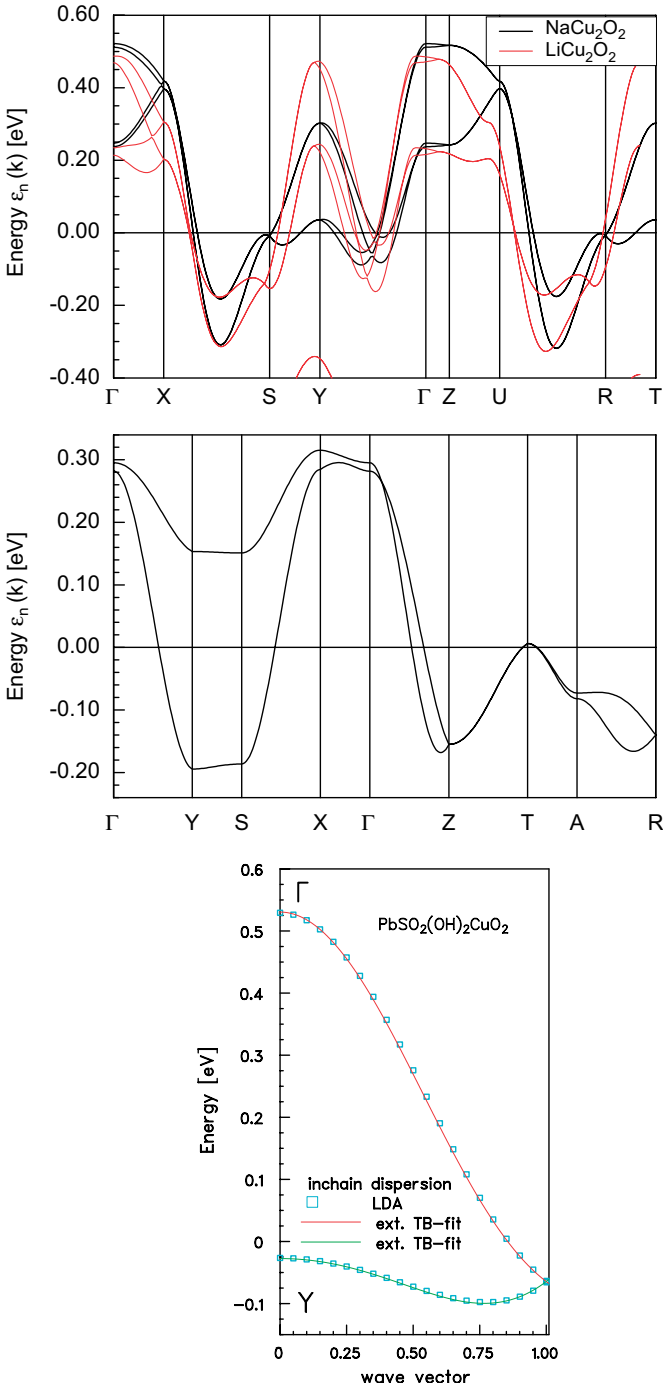

Fig. 4. Comparison of LDA–FPLO band structures for the isomorphic double chain compounds ACu_2O_2, A = Li, Na, (upper panel), Li_2ZrCuO_4 (middle panel), and $Pb[Cu(SO_4)(OH)_2]$ (lower panel) $\Gamma, X, Y, Z, \ldots$ is the standard wave vector notation for symmetry points $(0,0,0); (2\pi/a,0,0); (0,2\pi/b,0); (0,0,2\pi/c); \ldots$, respectively.

the IC magnetic structure under consideration. In this context, for $LiCu_2O_2$ two alternative frustration models have been employed interpreting the inelastic neutron scattering and other experimental data: (i) the "AF-M–AFM"–DC (AA-dc) or dimer liquid model [5,24,25] and (ii) the isotropic FM–AFM single-chain J_1-J_2 model (FA-sc-J_1J_2) [6–8]. In the meantime model (ii) has been widely accepted [22,23,10] as a reasonable starting point especially supported also by new results for the isomorphic compound $NaCu_2O_2$ [11–13] except recent ARPES data for $LiCu_2O_2$ described within an unfrustrated 1D spinon–holon picture [26] whose microscopic interpretation remains rather unclear (see Section 2). For $NaCu_2O_2$ as a slight modification of model (ii): a frustrated FAAA J_1-J_4 model with two added AFM long-range exchanges J_3 and J_4 has been proposed [11].

Finally, based on a low-T fit of $\chi(T)$ Hase et al. [27] adopted the FA-sc-J_1J_2-model (ii) also for $Rb(Cs)_2Cu_2Mo_3O_{12}$. Above 2 K no magnetic ordering has been detected. But for Li_2ZrCuO_4 (see Fig. 3) [28] and for $Pb[Cu(SO_4)(OH)_2]$ (see Fig. 4) a yet unresolved magnetically ordered state might occur below 6 K and 2.7–2.8 K, respectively suggested by a sharp specific heat anomaly and a maximum of $d(\chi(T)T)/dT$ [29].

2. Crystal structure and basic electronic structure of helimagnetic chain cuprates with acute pitches

Before turning to electronic and magnetic properties we would like to remind the reader about common and specific structural features for each of the considered compounds. The commonly used chemical notation is somewhat misleading because it does not reflect properly the cuprate and the CuO_2 chain character which, however, dominates the low-energy electronic and the magnetic properties. For instance, according to the orbital analysis of states near the Fermi energy using the FPLO–LDA band structure code [30], transition metal ions, except Cu, do enter magnetically inert complex cations to compensate the anionic cuprate units. Thus, $LiCuVO_4$ (Fig. 1) is not a vanadate but a lithium vanadyl cuprate which should be written more correctly as $[LiVO_2]^{2+}[CuO_2]^{2-}$. In this compound V is almost in a cationic V^{5+} state with unoccupied 3*d* and 4*s* shells and therefore it is magnetically silent. Similarly, as Zr and Mo in Li_2ZrCuO_4 and $Rb(Cs)_2Cu_2Mo_3O_{12}$, respectively, exhibit unfilled 4*d* and 5*s* shells and are therefore found in cationic 4+ and 6+ states. In $Li(Na)Cu_2O_2$ there are two Cu sites: one in the chains is 2+ and magnetically active whereas a second one in between (see Fig. 2) is 1+ and magnetically silent. Finally, Pb in $Pb_2[CuSO_4(OH)_2]$ is in the cationic 4+ state with a filled 5*d* shell. Taking into account the strong correlation effects for Cu^{2+} compounds it becomes clear that all these undoped cuprates are charge transfer insulators with correspondingly large gap values in the order of $\Delta_{pd} \sim 3-4$ eV or even larger. However, the observed smaller optical gap $E_g \approx 1.95$ eV in $LiCu_2O_2$ [26] results probably from transition into an empty Cu(1) derived band lying inside the larger charge transfer gap of the $Cu(2)O_2$ chains in contrast to the charge transfer assignment suggested in Ref. [26]. The large holon and spinon dispersions of $2t_{\mathrm{eff}} \approx 0.74$ eV and $0.5\pi J_{\mathrm{eff}} \approx 55$ meV, respectively, found there cannot be understood neither from the relative small band width of the half-filled cuprate band at the Fermi energy (see Fig. 4) within the

LDA which amounts for all edge-shared CuO_2 compounds under consideration 0.5–0.8 eV, only, nor from a simple internal self-consistency. In fact, adopting a standard value for the effective *one-band* (!)Hubbard $U\sim 3-4$ eV instead of the $U_{dd}\sim 8$ eV (appropriate only for a *multi*(five)band-*pd* Hubbard model), one would arrive at $J_{\rm eff}=4t_{\rm eff}^2/U\leqslant$ 136 meV, a value exceeding by an order of magnitude the commonly accepted value for the most AFM edge-shared CuO_2 compound $CuGeO_3$.

3. Low-field properties and weak ferromagnetism

This disparity in transition temperatures T_h, pitches, the possible subsequent occurrence of weak ferromagnetism below T_h, or the absence of any ordering at low T results from a complex interplay between the strength of frustration, the actual internal anisotropy of inchain and perpendicular transfer integrals governed by the chain geometry including the Cu–O–Cu bond angle $\gamma\sim 90^\circ$, the exchange anisotropy affected by local distortions from the ideal flat chain-geometry, the strength of the crystal field affected by the position and the charge of the cations, as well as the nature and the strength of the interchain coupling. $Rb(Cs)_2Cu_2Mo_3O_{12}$ shows strongly distorted non-planar chains formed by an unusual asymmetric (non-diagonal!) corner-sharing of CuO_4-plaquettes with a Cu–O–Cu NN bond angle of 103° (see Fig. 3). The arrangement of NNN plaquettes resembles that in edge-shared CuO_2 chains pointing to an AFM J_2, whereas the FM nature of J_1 is similar to that for the strongly buckled rungs in the pseudo-ladder compound $MgCu_2O_3$ with an angle $\gamma\approx 108^\circ$ [31]. Then $J_1\sim -10$ to -30 meV can be estimated. Adopting the same order of $J_2\sim 5-10$ meV as for edge-shared CuO_2-chains one arrives at parameters comparable with Li_2ZrCuO_4 [28]. For this reason we included $Rb(Cs)_2Cu_2Mo_3O_{12}$ in our phenomenological analysis too [32].

Susceptibility $\chi(T)$ and magnetization measurements combined with specific heat $c_p(T,H)$ data provide useful insight in the basic spin–spin interactions. Thus, the shape of $\chi(T)$ together with the Curie–Weiss temperature $\Theta_{\rm CW}^{\rm 1D}$ obtained from its high-temperature asymptotics yield constraints for the strength of frustration and the contribution of residual interchain exchange. Typical shapes of $\chi(T)$ together with fits by the FA-sc-J_1J_2-model for $NaCu_2O_2$ are shown in Fig. 5. A systematic evolution of the empirical maximum positions $T_{\rm max}^{\chi}/J_2$ in units of J_2 of the same model applied to related systems is shown in Fig. 6 [33]. Our analysis of $\chi(T)$ and c_p for polycrystalline Li_2ZrCuO_4 [28] yields $\alpha\approx 0.28-0.3$, i.e. a value rather close to the quantum critical point $\alpha_c=\frac{1}{4}$ (the spiral-FM transition). To the best of our knowledge, at present Li_2ZrCuO_4 is the most critical system from the helical side. It deserves more detailed investigation in future. In Fig. 6 also the predictions for $T_{\rm max}^{\chi}/J_2$ within the

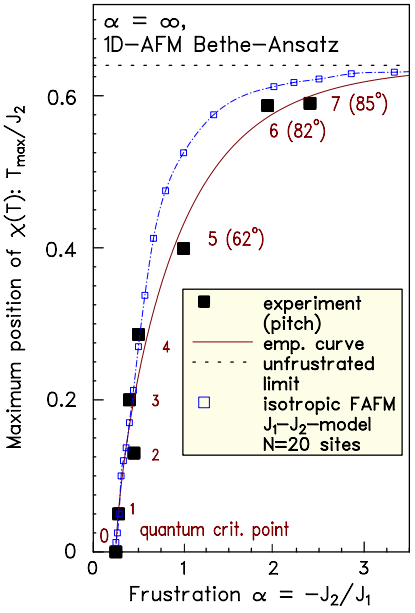

Fig. 6. Maximum temperature of $\chi(T)$ in units of the estimated NNN inchain exchange integral J_2 of the FA-sc-J_1J_2-model vs. the inchain frustration parameter $\alpha=-J_2/J_1$ for various edge-shared chain cuprates. The numbers denote the compounds: 1—Li_2ZrCuO_4, 2—$Pb_2[CuSO_4(OH)_2]$, 3—$Rb_2Cu_2Mo_3O_{12}$, 4—$Cs_2Cu_2Mo_3O_{12}$, 5—$LiCu_2O_2$, 6—$NaCu_2O_2$, 7—$LiCuVO_4$.

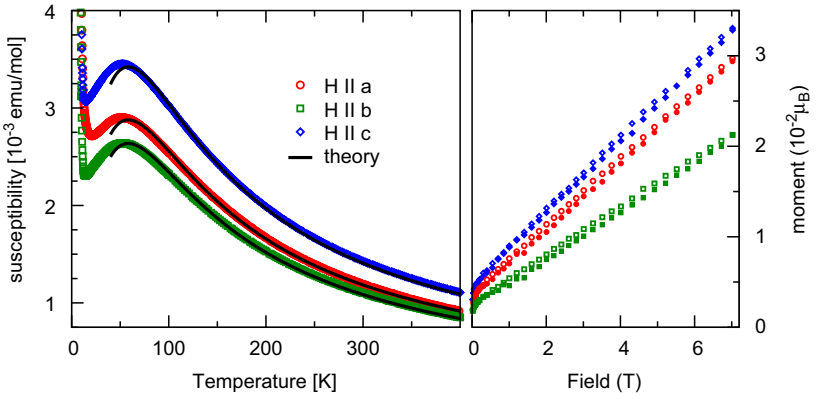

Fig. 5. Theoretical spin-susceptibility $\chi(T)$ for large periodic spin-1/2 FM-AFM Heisenberg chains with $N=16$ sites compared with experiments for $NaCu_2O_2$ taken from Ref. [12] (left panel). Magnetization vs. applied field at $T=2$ K (right panel).

FA-sc-J_1J_2-model are shown as derived from full diagonalizations of periodic rings with $N = 20$ sites using own results [28] as well as Ref. [34], both being in accord with the transfer matrix renormalization group results of Ref. [35] taken as estimates for $N = \infty$. Thus we may conclude that our FA-sc-J_1J_2-model yields an excellent starting point for the considered chain cuprates. Despite small corrections due to possible exchange anisotropy and doping effects caused by small deviations from stoichiometry in real compounds the general good unified description clearly supports our point of view that the compounds under consideration in fact belong to a special subclass of chain cuprates different from the "FM" Li_2CuO_2 and the well-known AFM spin-Peierls system $CuGeO_3$.

The staggered tilting of CuO_4 plaquettes of all four non-planar (buckled) chain compounds Li_2ZrCuO_4, $Pb_2[CuSO_4(OH)_2]$, and $Rb(Cs)_2Cu_2Mo_3O_{12}$ as well as within the bilayers of $Na(Li)Cu_2O_2$ may cause along a-axis oscillating terms in $\mathscr{H}$ and this way a staggered field induced magnetization which yields a spin gap Δ_s for one of the two acoustic branches near Γ, akin to the mechanism proposed for Cu-benzoate at the 1D Brillouine zone (BZ) boundary [36]. A field dependent Δ_s could explain the field sensitivity of c_p at moderate H seen in $NaCu_2O_2$.

Another interesting point is the weak hysteresis which occurs in $NaCu_2O_2$ below $T^* \approx 8-9.5$ K, well below the spiral ordering at $T_h = 13$ K (see Figs. 5, 7). The observed local moment $M_0 \approx 4 \times 10^{-3}\,\mu_B$ at $T = 2$ K is a typical value for other weak FM cuprates. The weak ferromagnetism can be ascribed to the presence of DM exchange allowed in $NaCu_2O_2$. In fact, the inspection of the local structure of the slightly tilted CuO_4 plaquettes reveals a shift of the Cu^{2+} ion off from the plaquette center (Fig. 2) which might explain the origin of DM [37]. Alternatively, it might point to a secondary phase transition induced by the increasing spiral order parameter with decreasing T. In this way, strong enough local magnetic moments induced by the spiral formation visualize finally the broken inversion symmetry of a single CuO_2 chain at $T \leqslant T^* < T_h$ and allow the smooth occurrence of strong enough DM exchange and weak FM below T^* only. Finally, we note that, in principle, a symmetric exchange anisotropy [10] might explain the spiral orientation and according to Ref. [38] for $\alpha \gg 1$ (only roughly fulfilled here) also the occurrence of chiral structures coexisting with ferromagnetism. This might be of relevance in the context of a much weaker induced FM moment at the limits of experimental error bars in the isomorphic $LiCu_2O_2$ [39] which exhibits $\alpha \approx 1$ only [6–8].

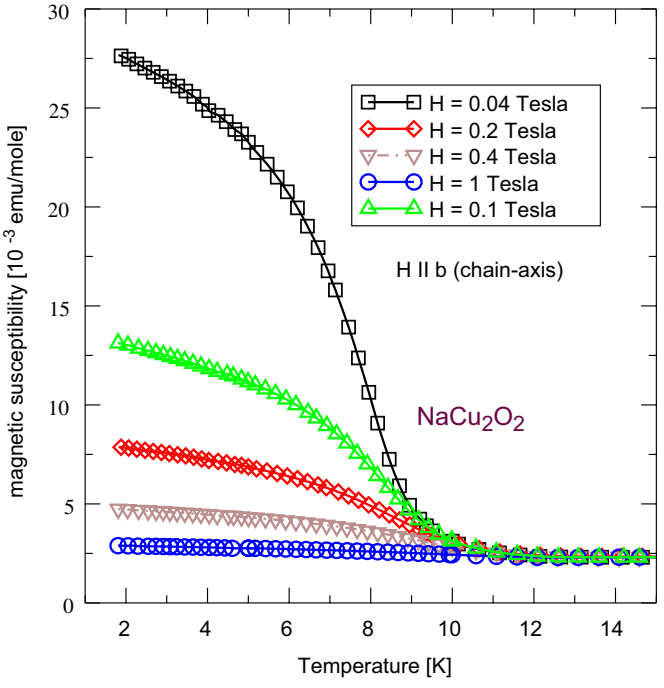

Fig. 7. Low temperature spin-susceptibility $\chi(T)$ for different magnetic fields H applied in chain direction.

4. The high-field magnetization and the search for novel commensurate quantum phases

Some details of the magnetic spiral, especially its evolution under applied external magnet fields, are still unclear. However, the small exchange integrals obtained for $LiCuVO_4$ allow the determination of the field dependent magnetization up to the saturation field $H_s \sim 40-50$ T [4] when all spins are aligned (at $T = 0$). Remarkably, for the FA-sc-J_1J_2-model even with some further extensions H_s can be found analytically [40], this way providing a useful constraint for the J-values. Moreover, these calculations point to a novel physical picture dominated by bound two-magnon states at least at high fields $H \leqslant H_s$. In particular, it was found for large but finite systems that there the magnetization determined by exact full diagonalizations (see Fig. 8) or applying the powerful DMRG-technique [34] changes in steps of $\Delta S_z = 2$ unlike the usual one-magnon behavior where $\Delta S_z = 1$. Based on approximate mean-field (MF) calculations a related novel commensurate period-4 collinear quantum phase above the conic spiral phase for weak and medium fields has been predicted [41]. In Ref. [4], the classical saturation field $g\mu_B H_s^{cl} = 2J_2(1 - 0.25/\alpha)^2$ determined by the one-magnon instability of the fully aligned FM state has been ascribed to the maximum of dM/dH which for $H \| c$ amounts about 41 T (see Fig. 8). However, the true quantum spin-$\frac{1}{2}$ saturation field $g\mu_B H_s = 2J_2(1 - 0.25/\alpha^2 - 0.5/\alpha)/(1 - 1/\alpha)$ derived from the two-magnon instability of the fully aligned FM state [42,40] yields $H_s \approx 50$ T using J_1 and J_2 from our $\chi(T)$-fit in reasonable accord with experiment. Anyhow, within the numerical calculations no jump in the magnetization near 41 T could be detected. In accord with the statement given in Ref. [34] that for $\alpha \gg 1$ practically the whole field region is determined by the two-magnon sector. Fig. 8 shows that this peculiar quantum effect holds also already for $\alpha = 2.39$ and for a realistic symmetric anisotropy of the expected easy-axis type [43]. Thus, we are forced to conclude that both exactly treated pure 1D

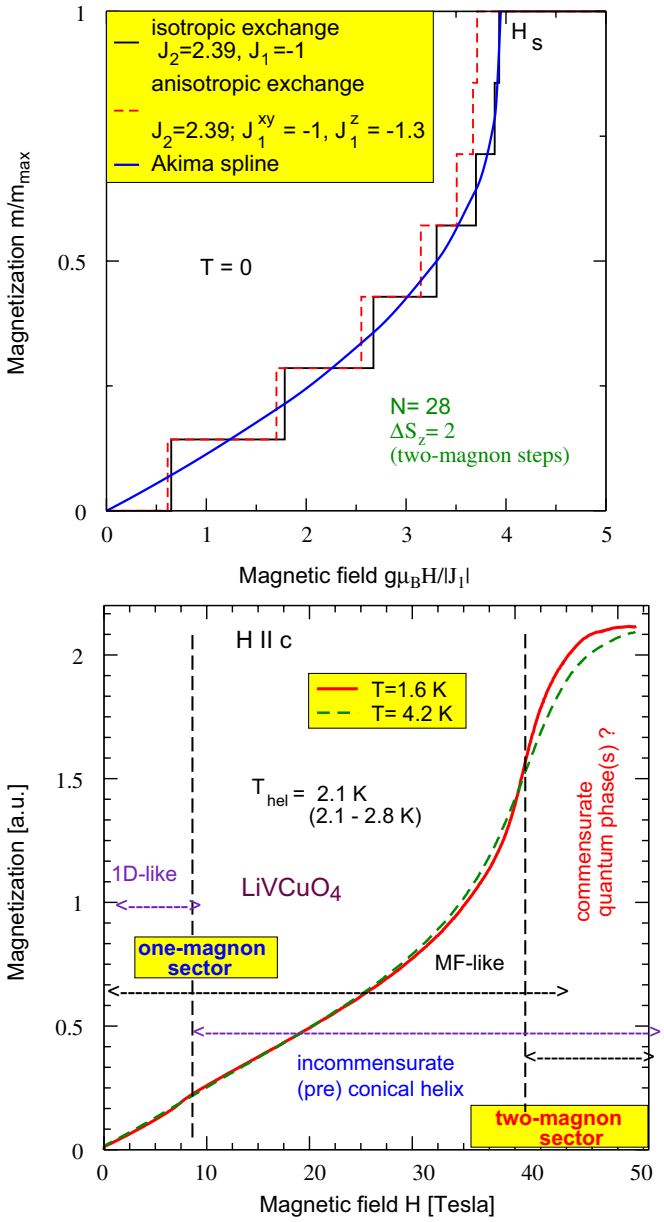

Fig. 8. Upper panel: magnetization vs. applied magnetic field at $T = 0$ for a long periodic chain with $N = 28$ sites within the easy-axis anisotropic and isotropic FA-sc-J_1J_2-models. Lower panel: experiment: $LiVCuO_4$ and possible scenarios beyond 1D.

models as well as simple MF-like approaches fail to describe the strong, nearly symmetric maximum in dM/dH near 41 T below H_s. On the other hand, there is no long-range spiral phase in 1D according to the Mermin–Wagner theorem. We expect that the present finite interchain exchange responsible for the observed finite T_h near 3 K [3,4] at $H = 0$ is also responsible for a strong reduction of the two-magnon dominated collinear commensurate phase. As a result, in the real quasi-1D situation a "crossover" between the predicted extremely broad 1D region $\Delta H_{1D}\sim 50$ T and the narrow mean field region $\Delta H_{mf}\sim 1$ T broad region for the novel quantum two-magnon collinear commensurate phase estimated as $\Delta H_{q1D}\sim 5$ T from Fig. 8 is realized. Interestingly, a failure of the 1D isotropic FA-sc-J_1J_2-model was mentioned by Lu et al. [35] for the description of the high-field magnetization of $Rb(Cs)_2Cu_2Mo_3O_{12}$. They ascribed it to missing DM exchange suggested by the low symmetry generic for buckled chains (see Fig. 3). Since in our case, with flat CuO_2 chains, there is no reason for a significant DM exchange, we suggest that an interchain scenario as considered here might contribute also to that failure. In this context it should be noted that near the FM critical point the 1D contribution to the saturation field H_s is small by definition. Hence, the $M(H)$ measurements at high fields might mainly probe the AFM interchain exchange. Thus, the situation is much different from the cases of fitting $\chi(T)$ and $c_p(T)$ which are dominated by strong sharp peaks at low T in accord with the predictions of the FA-sc-J_1J_2-model [28,34,35].

5. Frustration from multiband Hubbard models and the role of interchain interaction

If one takes into account only NN and NNN exchange, for AFM coupling $J_2 > 0$ along a single CuO_2 chain, one is left with a frustration problem irrespective of the sign of J_1. For Li_2CuO_2, where many experimental data are available, we fitted an extended five band Hubbard-model to describe the optical conductivity and O 1s X-ray-absorption data. Then the low-energy states of small Cu_nO_{2n} clusters have been mapped onto the corresponding clusters of the FA-sc-J_1J_2-model. As a result one arrives at a significant AFM NNN exchange integral due to a non-negligible NNN transfer integral t_{2y} leading to $\alpha = 0.7$. However, such a large value of α clearly exceeds the well-known critical value of $\alpha_c^{1D} = \frac{1}{4}$ for a spiral instability. This seeming contradiction with ENS data which show a FM inchain ordering can be resolved taking into account the non-negligible specific interchain coupling in Li_2CuO_2 [7,14]. In $LiVCuO_4$ and $Na(Li)Cu_2O_2$, the interchain coupling only weakly affects α_c since according to Refs. [4,6,12] it is not frustrated. Here, the in-phase arrangement of chains slightly reduces the effective FM NN J_1.

6. Summary

To conclude, we have shown that the FA-sc-J_1J_2 model supplemented with realistic interchain couplings from band structure calculations and small exchange anisotropies to explain the observed weak ferromagnetism reveals a proper description at low magnetic fields of various edge-shared CuO_2 chain compounds. The detailed understanding of the detected spiral states and the search of novel quantum phases, especially under high magnetic fields, remain challenging issues for future work.

Although all considered compounds exhibit rather different FM NN inchain exchange couplings: $J_1 = -1.8$ to -40 meV, the NNN counter part differs only by a factor of two or three with J_2 in between 4 and 11 meV. Li_2CuO_2

is found to be very close to a FM–AFM helical in-chain ground state still prevented by a strong specific, frustrated interchain coupling, whereas the long sought "FM" spin-$\frac{1}{2}$ helix with an acute pitch is realized in $LiCuVO_4$ and $Li(Na)Cu_2O_2$ and possibly also in Li_2ZrCuO_4 and $Pb_2[CuSO_4(OH)_2]$. Concerning $Rb(Cs)_2Cu_2Mo_3O_{12}$, a finite T_h might be still observed around 2 K. Other members of this fascinating family will be considered elsewhere.

Acknowledgments

The DFG, 486 RUS 113, KL 1824 (Emmy-Noether-program), GIF (I-811-237.14103), INTAS, CRDF JSTC 3501, and RFBR (06-02-16088, 07-02-91201, 07-02-00350) are acknowledged for financial support.

Note added in Proof

Since the original submission of the manuscript (June 24, 2006) the research field of FM frustrated edge-shared CuO_2 chain compounds has been rapidly developed. Hence, we would like to inform the reader about recently published results: (i) the observation of ferroelectricity in the spiral phases of $LiVCuO_4$ and $LiCu_2O_2$ by Y. Naito *et al.* J. Phys. Soc. Jpn. 76 (2007) 023708 and S. Park *et al.*, Phys. Rev. Lett. 98 (2007) 057601, respectively, (ii) a new theoretical analysis of exchange integrals in $LiCu_2O_2$ by V. Mazurenko *et al.*, cond-mat/0702276 (2007), (iii) an interpretation of the same high-field magnetization data of $LiVCuO_4$ as shown in Fig. by M.G. Banks *et al.*, J. Phys. Cond. Mat. 19(2007) 145227 as well as (iv) the observation of an unusual strong field dependence of the specific heat in Li_2ZrCuO_4 [28].

Due to the lack of space we may only briefly comment some aspects directly related to the present paper. The microscopic reason for the observed effect (i) remains unclear especially with respect to uncertainties/discrepancies of the approximately known magnetic spin structure of the helix [5]. Using LMTO and an LSDA + U calculations the authors of Ref. (ii) arrive at somewhat different values of the ferromagnetic J_1 and the antiferromagnetic J_2 exchange integrals as compared with our first analysis [6] (aimed at this early stage only to a proper prediction of their signs and the elucidation of the main origin of the frustration) and the later phenomenological analysis of the $\chi(T)$ data [8]. Anyhow, V. Mazurenko *et al.*, do confirm our result that the interchain coupling within one double chain of $LiCu_2O_2$ is very weak at variance with the result of the spin wave analysis of the neutron date given in Refs. 22,23. Concerning the slight cusp seen near 8 K in the magnetization data of $LiVCuO_4$, the authors of Ref. (iii) suggest in accord with our "1D-like scenario" an upper limit for the field induced instability of the ordinary helix. Finally, the strong field dependence of the specific heat and the shape of the low temperature peak near 6 K reported in Ref. 28 can be explained by the vicinity of Li_2ZrCuO_4 close to the quantum critical point near the ferromagnetic-spiral-transition.

References

[1] S. Ebisu, et al., J. Phys. Chem. Solids 59 (1998) 1407.
[2] E.M.L. Chung, et al., Phys. Rev. B 68 (2003) 144410.
[3] B.J. Gibson, et al., Physica B 350 (2004) E253.
[4] M. Enderle, et al., Europhys. Lett. 70 (2005) 237.
[5] T. Masuda, et al., Phys. Rev. Lett. 92 (2004) 177201.
[6] A.A. Gippius, et al., Phys. Rev. B 70 (2004) R01426.
[7] S.-L. Drechsler, et al., Phys. Rev. Lett. 94 (2005) 039705.
[8] S.-L. Drechsler, et al., J. Magn. Magn. Mater. 290 (2005) 345.
[9] A.A. Gippius, et al., J. Magn. Magn. Mater. 300 (2006) e335.
[10] M. Mihaly, et al., Phys. Rev. Lett. 97 (2006) 067206.
[11] L. Capogna, et al., Phys. Rev. B 71 (2005) R140402.
[12] S.-L. Drechsler, et al., Europhys. Lett. 73 (2006) 83.
[13] K.-Y. Choi, et al., Phys. Rev. B 73 (2006) 094409.
[14] Y. Mizuno, et al., Phys. Rev. B 57 (1998) 5326.
[15] M. Yamaguchi, et al., J. Phys. Soc. Japan 65 (1996) 2998.
[16] A.N. Vasil'ev, et al., Phys. Rev. B 64 (2001) 024419.
[17] Ch. Kegler, et al., Eur. Phys. B 22 (2001) 321.
[18] H.-A. Krug von Nida, et al., Phys. Rev. B 65 (2003) 134445.
[19] Y. Maeda, et al., Phys. Rev. Lett. 95 (2005) 037602.
[20] Ch. Kegler, et al., Phys. Rev. B 73 (2006) 104418.
[21] D. Dai, et al., Inorg. Chem. 43 (2004) 4026.
[22] T. Masuda, et al., Phys. Rev. Lett. 94 (2005) 039706.
[23] T. Masuda, et al., Phys. Rev. B 72 (2005) 014405.
[24] S. Zvyagin, et al., Phys. Rev. B 66 (2000) 064424.
[25] K.-Y. Choi, et al., Phys. Rev. B 69 (2004) 104421.
[26] M. Papagno, et al., Phys. Rev. B 73 (2006) 115120.
[27] M. Hase, et al., Phys. Rev. B 70 (2005) 10426;
M. Hase, et al., J. Appl. Phys. Lett. 97 (2005) 10B303.
[28] S.-L. Drechsler, et al., Phys. Rev. Lett. 98 (2007) 077202.
[29] M. Baran, et al., Phys. Stat. Sol. (c) 3 (2006) 220.
[30] K. Koepernik, H. Eschrig, Phys. Rev. B 59 (1999) 1743.
[31] S.-L. Drechsler, et al., Physica C 408 (2004) 270.
[32] Due to the incomplete structural data a band structure analysis of the J's cannot be performed for $Cs_2Cu_2Mo_3O_{12}$ at present.
[33] We note that the J-values for $Rb(Cs)_2Cu_2Mo_3O_{12}$ have been slightly changed compared with the values of low temperature fits reported in Refs. [27,28] using also the reported FM Curie–Weiss temperatures and adopting a weak interchain interaction of about 1 meV with two neighboring chains [28].
[34] F. Heidrich-Meisneret, et al., Phys. Rev. B 74 (2006) 020403.
[35] H.T. Lu, et al., Phys. Rev. B 74 (2006) 134425.
[36] M. Oshikawa, et al., Phys. Rev. Lett. 79 (1997) 2886.
[37] The nearly c orientation of the main DM-vectors might explain the observed nearly (ab) orientation of the helix. In a rigorous sense, we expect a more complex spin structure with two alternatingly tilted helices from each bilayer boundary. Using the fitted g_c and J_1 we estimate the NN DM vector as $|\mathbf{D}_{i,i+1}| = (\Delta g_c/g)\,|J_1| \sim 0.5$ meV. For more details see Ref. [12].
[38] M. Zarea, et al., Eur. Phys. J. B 39 (2004) 1434.
[39] R. Klingeler, private communication.
[40] R. Kuzian, S.-L. Drechsler, Phys. Rev. B 75 (2007) 024401.
[41] D. Dmitriev, V. Krivnov, Phys. Rev. B 73 (2006) 024402.
[42] A. Chubukov, Phys. Rev. B 44 (1991) 4693.
[43] V. Yushankai, R. Hayn, Europhys. Lett. 47 (1999) 116.